

# Thermalization of Heavy Quarks in the Quark-Gluon Plasma

Hendrik van Hees and Ralf Rapp

*Cyclotron Institute, Texas A&M University, College Station, Texas 77843-3366, USA*

(Dated: May 23, 2019)

Charm- and bottom-quark rescattering in a Quark-Gluon Plasma (QGP) is investigated with the objective of assessing the approach towards thermalization. Employing a Fokker-Planck equation to approximate the collision integral of the Boltzmann equation we augment earlier studies based on perturbative parton cross sections by introducing resonant heavy-light quark interactions. The latter are motivated by recent QCD lattice calculations which indicate the presence of “hadronic” states in the QGP. We model these states by colorless (pseudo-) scalar and (axial-) vector  $D$ - and  $B$ -mesons within a heavy-quark effective theory framework. We find that the presence of these states at moderate QGP temperatures substantially accelerates the kinetic equilibration of  $c$ -quarks as compared to using perturbative interactions. We also comment on consequences for  $D$ -meson observables in ultra-relativistic heavy-ion collisions.

PACS numbers: 12.38.Mh,24.85.+p,25.75.Nq

## I. INTRODUCTION

Hadrons containing heavy quarks are valuable probes of the strongly interacting matter produced in high-energy collisions of heavy nuclei. The spectral properties of (bound)  $c\bar{c}$  states, such as their binding energy and (decay) width, are expected to undergo substantial modifications in a Quark-Gluon Plasma (QGP) and thus affect charmonium yields and momentum spectra in heavy-ion reactions with QGP formation (see, *e.g.*, Ref. [1, 2, 3] for overviews). Reinteractions of *individual*  $c$ -quarks in the QGP will reflect themselves in transverse-momentum ( $p_T$ -) spectra of open charm hadrons ( $D$ -mesons), most notably their elliptic flow,  $v_2(p_T)$ , in semi-central collisions [4, 5]. Preliminary experimental results from the Relativistic Heavy-Ion Collider (RHIC) indicate the possibility that the  $D$ -meson  $v_2$  could be similar in magnitude to the one of light hadrons [6, 7]. Since the  $c$ -quark is rather heavy, this would be quite remarkable and could provide important insight into (nonperturbative) properties of the QGP at moderate temperatures,  $T \simeq 1$ - $2 T_c$ . *E.g.*, in the light-quark sector, parton rescattering through hadron-like states in the QGP (motivated by recent lattice calculations of Quantum Chromodynamics (QCD) at finite temperature) has been suggested as a mechanism to enhance partonic cross sections [8, 9, 10] in order to facilitate rapid thermalization of the bulk matter at RHIC as required in hydrodynamical models. The notion of charmonium resonances in the QGP [11, 12] has been applied earlier to assess  $J/\psi$  production at SPS and RHIC [15]. Employing kinetic rate equations to consistently account for both dissociation and regeneration reactions,  $c + \bar{c} \leftrightarrow J/\psi + X$ ,  $J/\psi$  resonance formation in the QGP via  $c\bar{c}$  “coalescence” turns out to be the dominant contribution to the final yield in central  $Au$ - $Au$  collisions at RHIC [13, 14, 15] (see also Refs. [16, 17]). Furthermore,  $J/\psi$  production was found to be sensitive to the in-medium properties of charm quarks, *i.e.*, their in-medium masses and degree of kinetic equilibration [15, 18, 19].

Early studies of charm-quark thermalization in the QGP have been conducted in Ref. [20] based on elastic perturbative cross sections [21],  $c + q(\bar{q}, g) \rightarrow c + q(\bar{q}, g)$ , implemented into a Fokker-Planck equation to approximate the collision integral of the Boltzmann equation. With a strong coupling constant  $\alpha_s=0.6$  rather short relaxation times of around  $\sim 4$  fm/ $c$  have been found for a massless QGP at temperatures  $T \simeq 400$  MeV. However, since the relaxation times are essentially proportional to  $\alpha_s^{-2}$ , more moderate values of  $\alpha_s$  (*e.g.*, 0.3) lead to a significant decrease (factor

3-4), rendering thermalization of  $c$ -quarks under RHIC conditions unlikely. This is consistent with recent transport studies [22, 23].

In the present article we evaluate heavy-quark rescattering in the QGP via “ $D$ ”- and “ $B$ ”-meson resonances, the existence of which is the main assumption in our work. Although lattice QCD has not yet addressed in-medium heavy-light ( $Q$ - $\bar{q}$ ) spectral functions at finite temperature, resonance-like correlations in the QGP are quite plausible in view of the indications for both  $q$ - $\bar{q}$  and  $Q$ - $\bar{Q}$  systems. Further support for this assumption is provided by calculations using effective four-quark interactions within Nambu-Jona-Lasinio models [24, 25, 26]. With form factors and coupling constants adjusted to free  $D$ -meson masses, finite-temperature calculations lead to resonances above the  $Q$ - $\bar{q}$  threshold in the QGP, with appreciable widths of several hundred MeV.

Our article is organized as follows: in Sec. II we introduce Lagrangians for resonant  $c$ - $q$  interactions based on chiral and heavy-quark symmetry for pseudo-/scalar and axial-/vector multiplets (Sec. II A) and evaluate pertinent scattering amplitudes (Sec. II B). In Sec. III we apply the resulting cross sections within a Fokker-Planck equation; we first determine temperature and momentum dependencies of drag and diffusion constants in a static QGP (Sec. III A), and then evaluate the time evolution of  $c$ -quark transverse-momentum ( $p_T$ ) spectra within an expanding fireball model to simulate conditions in heavy-ion collisions at RHIC (Sec. III B). We conclude in Sec. IV including a discussion on open-charm observables in URHIC’s.

## II. $D$ -MESONS IN THE QUARK-GLUON PLASMA

### A. Heavy-Light Quark Lagrangians

Our description of  $D$ -meson resonances in the QGP is based on a rather simplistic quark-meson model, accounting, however, for the relevant symmetries, *i.e.*, chiral symmetry in the light quark sector ( $u$ - $d$ ) and heavy-quark symmetry for  $c$ -quarks. As a minimal set of resonances, consistent with lattice calculations [27], we assume the lowest-lying pseudoscalar ( $D$ ) and vector mesons ( $D^*$ ) to survive above  $T_c$ <sup>1</sup>. In addition, (approximate) restoration of chiral symmetry mandates the existence of pertinent  $SU(2)_f$  chiral partners in the scalar ( $D_0^*$ ) and axial-vector ( $D_1$ ) channel with mass and width identical to  $D$  and  $D^*$ , respectively. The effective Lagrangian thus takes the form

$$\begin{aligned} \mathcal{L}_{Dcq} = & \mathcal{L}_D^0 + \mathcal{L}_{c,q}^0 - iG_S \left( \bar{q}\Phi_0^* \frac{1+\not{p}}{2} c - \bar{q}\gamma^5 \Phi \frac{1+\not{p}}{2} c + h.c. \right) \\ & - G_V \left( \bar{q}\gamma^\mu \Phi_\mu^* \frac{1+\not{p}}{2} c - \bar{q}\gamma^5 \gamma^\mu \Phi_{1\mu} \frac{1+\not{p}}{2} c + h.c. \right) \end{aligned} \quad (1)$$

with the usual free (kinetic and mass) terms for quarks and  $D$ -mesons,

$$\begin{aligned} \mathcal{L}_{c,q}^0 &= \bar{c}(i\not{\partial} - m_c)c + \bar{q}i\not{\partial}q, \\ \mathcal{L}_D^0 &= (\partial_\mu \Phi^\dagger)(\partial^\mu \Phi) + (\partial_\mu \Phi_0^{*\dagger})(\partial^\mu \Phi_0^*) - m_S^2 (\Phi^\dagger \Phi + \Phi_0^{*\dagger} \Phi_0^*) \\ &\quad - \frac{1}{2} (\Phi_{\mu\nu}^{*\dagger} \Phi^{*\mu\nu} + \Phi_{1\mu\nu}^\dagger \Phi_1^{\mu\nu}) + m_V^2 (\Phi_\mu^{*\dagger} \Phi^{*\mu} + \Phi_{1\mu}^\dagger \Phi_1^\mu). \end{aligned} \quad (2)$$

The fields  $\Phi$  represent *anti*- $D$ -mesons, transforming as isospinors under isospin rotations.

The interaction terms in Eq. (1) will be evaluated to leading order in  $1/m_c$  according to heavy-quark effective theory (HQET) [28]. This ensures the absence of unphysical (4-D longitudinal)

---

<sup>1</sup> In the vacuum these are associated with  $D^+$ (1870),  $D^0$ (1865) and  $D^*$ (2010) mesons.

degrees of freedom for massive (axial-) vector meson fields as encoded in the transversality constraints

$$v_\mu \Phi^{*\mu} = v_\mu \Phi_1^\mu = 0 \quad (3)$$

( $v_\mu$ : four velocity of the charm quark or  $D$ -meson). Equivalent relations hold for the  $D$ -meson self-energies (to leading order in the  $1/m_c$  expansion of HQET).

In the light-flavor sector the relevant symmetry is the invariance of the Lagrangian under the chiral  $SU(2)_L \times SU(2)_R$  group. For infinitesimal angles  $\delta\vec{\phi}_{V,A}$ , it is characterized by the standard vector and axial-vector transformations acting on the quark fields as

$$q \rightarrow (1 + i\delta\vec{\phi}_V \vec{t} + i\delta\vec{\phi}_A \vec{t}\gamma_5)q, \quad c \rightarrow c \quad (4)$$

with  $\vec{t} = \vec{\tau}/2$  the generators of  $SU(2)$  ( $\vec{\tau}$ : Pauli matrices). To construct the group operations for the  $\bar{D}$  fields, we identify the latter with underlying quark currents according to

$$\Phi \sim \bar{c}\gamma_5 q, \quad \Phi_0^* \sim \bar{c}q, \quad \Phi_\mu^* \sim \bar{c}\gamma_\mu q, \quad \Phi_{1,\mu} \sim \bar{c}\gamma_\mu\gamma_5 q. \quad (5)$$

Here, “ $\sim$ ” denotes “transforms under (4) like”. Thus the transformation rules for the  $\bar{D}$ -meson fields follow as

$$\begin{aligned} \Phi &\rightarrow \Phi + i\delta\vec{\phi}_A \cdot \vec{t}\Phi + i\delta\vec{\phi}_V \cdot \vec{t}\Phi_0^*, \\ \Phi_0^* &\rightarrow \Phi_0^* + i\delta\vec{\phi}_A \cdot \vec{t}\Phi_0^* + i\delta\vec{\phi}_V \cdot \vec{t}\Phi. \end{aligned} \quad (6)$$

With these properties the Lagrangian, Eq. (1), is a scalar under chiral transformations.

For  $D_s$ -mesons we restrict ourselves to the (experimentally known) pseudoscalar and vector states since spontaneous chiral symmetry breaking in the strange-quark sector is expected to persist to temperatures significantly larger than  $T_c$  (characterized by sizable values of the strange condensate  $\langle \bar{s}s \rangle$ ). The corresponding Lagrangian is therefore taken to be

$$\begin{aligned} \mathcal{L}_s = & (\partial_\mu \Phi_s^\dagger)(\partial^\mu \Phi_s) - m_{D_s}^2 \Phi_s^\dagger \Phi_s - \frac{1}{2} \Phi_{s\mu\nu}^{*\dagger} \Phi_s^{\mu\nu} + m_{D_s^*}^2 \Phi_{s\mu}^{*\dagger} \Phi_s^\mu \\ & - iG_{s,S} \bar{s}\gamma^5 \Phi_s \frac{1+\gamma}{2} c - G_{s,V} \bar{s}\gamma^\mu \Phi_{s,\mu}^* \frac{1+\gamma}{2} c. \end{aligned} \quad (7)$$

Eqs. (1) and (7) constitute our basic vertices for effective charm-light quark interactions in the QGP (analogous expressions hold in the  $b$ -quark sector upon the replacement  $c \rightarrow b$  and  $D \rightarrow B$ ). The underlying parameters, *i.e.*, the bare masses of the  $D$ -meson and their coupling strength to the quarks, will be fixed to resemble more microscopic model calculations of corresponding spectral functions above  $T_c$ , as discussed below. In the following we will also impose the spin symmetry of HQET implying that the spectral properties of pseudoscalar and vector mesons, and consequently their masses and couplings to quarks, are equal.

## B. Meson Self-Energies and Heavy-Light Quark Scattering Amplitudes

The key ingredient for the heavy-quark scattering amplitudes are the heavy-meson exchange propagators,

$$D_{D,B}(k) = \frac{1}{k^2 - m_{D,B}^2 - \Pi_{D,B}(k)}, \quad (8)$$

which are essentially determined by the underlying self-energies,  $\Pi_{D,B}$ , together with the bare resonance masses,  $m_{D,B}$ , of the Lagrangian. In the following, we will evaluate the self-energies

in terms of the heavy-light-quark loop (cf. the left diagram in Fig. 1), thereby investigating two different schemes to regularize the divergent loop integrals to assess the robustness of our results. We will concentrate again on the charm-quark case, but completely analogous expressions apply to the bottom sector.

Within the dimensional regularization scheme (see, *e.g.*, [29]), the interaction vertices of Eq. (1) yield a self-energy for (pseudo-) scalar  $D$ -mesons of 4-momentum  $k$  of the form

$$\begin{aligned} \Pi_D(s) = \Pi_{D_0^*}(s) &= 3iG^2\mu^{4-d} \int \frac{d^d l}{(2\pi)^d} \text{Tr}[\gamma_5 G_q(l+k)\gamma_5 G_Q(l)] \\ &= \frac{3G^2}{8\pi^2} \left\{ \frac{4m_c^2 - 2s}{4-d} + 3m_c^2 - 2s + (s - 2m_c^2) \left[ \gamma + \ln \left( \frac{m_c^2 - s}{4\pi\mu^2} \right) \right] \right. \\ &\quad \left. + \frac{m_c^4}{s} \ln \left( \frac{m_c^2 - s}{m_c^2} \right) \right\}, \end{aligned} \quad (9)$$

( $s = k^2$ ). The first term contains the quadratic divergence for  $d \rightarrow 4$ , showing that the self-energy can be rendered finite with a field- and mass-renormalization;  $\mu$  denotes the mass scale in the dimensional-regularization scheme to keep the momentum dimensions of the integrals as for  $d = 4$ , and  $\gamma \simeq 0.577$  is Euler's constant. The (regularization-independent) imaginary part is given by

$$\text{Im } \Pi_D(s) = -\frac{3G_S^2}{8\pi} \frac{(s - m_c^2)^2}{s} \Theta(s - m_c^2). \quad (10)$$

For the vector and axial-vector mesons, we employ the HQET propagator for the charm quark,

$$G_v(l) = \frac{m_c}{m_c v \cdot l + i\eta} \frac{1 + \not{v}}{2}, \quad (11)$$

to obtain a transverse self-energy in leading order of the expansion in  $1/m_c$ . In Eq. (11), the “residual momentum”  $l$  of the charm quark is defined via its total 4-momentum as  $l_c = m_c v + l$ . For the  $D$ -meson fields the corresponding decomposition for the heavy-quark expansion reads

$$k_c = m_c v + k, \quad s = k_c^2 = m_c^2 \left[ 1 + \frac{2v \cdot k}{m_c} + \mathcal{O}\left(\frac{p^2}{m_c^2}\right) \right] \Rightarrow v \cdot k = \frac{s - m_c^2}{2m_c} + \mathcal{O}\left(\frac{p^2}{m_c^2}\right). \quad (12)$$

Applying the Feynman rules, and after some (Dirac) algebra, the dimensionally regularized polarization tensor for the axial-/vector becomes

$$\Pi_{D^*}^{\mu\nu}(p) = \Pi_{D_1}^{\mu\nu}(p) = -6iG_V^2\mu^{4-d}m_c \int \frac{d^d l}{(2\pi)^d} \frac{(l+p)_\nu v_\mu - (l+p) \cdot v g_{\mu\nu}}{[(l+p)^2 + i\eta](m_c v \cdot l + i\eta)}. \quad (13)$$

The integral is conveniently evaluated with help of the identity [30]

$$\frac{1}{ab} = \int_0^\infty d\lambda \frac{2}{(a + 2\lambda b)^2}. \quad (14)$$

Upon integrating over  $\lambda$  one obtains for the imaginary part

$$\text{Im } \Pi_{D^*}^{\mu\nu}(p) = \text{Im } \Pi_{D_1}^{\mu\nu}(p) = -(v_\mu v_\nu - g_{\mu\nu}) \frac{3G_V^2}{8\pi} \frac{(s - m_c^2)^2}{m_c^2} \Theta(s - m_c^2). \quad (15)$$

Since up to corrections  $\mathcal{O}(vk/m_c)$  one can identify  $m_c^2 = s$  in the denominator, one finds

$$\Pi_{D^* \mu\nu}(s) = \Pi_{D_1 \mu\nu}(s) = (v_\mu v_\nu - g_{\mu\nu}) \Pi_D(s), \quad (16)$$

which is the expected result from spin symmetry of the HQET. We define the renormalization constants for the self-energy by the following conditions,

$$\partial_s \Pi_D^{(\text{ren})}(s)|_{s=0} = 0, \quad \text{Re} \Pi_D^{(\text{ren})}(s)|_{s=m_D^2} = 0. \quad (17)$$

The first condition ensures that, within a vector dominance model, the photon propagator has residuum of unity at  $s = 0$ , while the second one implies that the renormalized meson mass coincides with the bare mass of the Lagrangian. The renormalized self-energy is, of course, independent of the dimensional-regularization scale  $\mu$ .

As an alternative way of regularizing the divergent self-energy integrals we introduce a dipole form factor at the  $c$ - $q$ - $D$  vertex,

$$F(|\vec{q}|) = \left( \frac{2\Lambda^2}{2\Lambda^2 + \vec{q}^2} \right)^2, \quad (18)$$

where  $\vec{q}$  denotes the 3-momentum of the quarks in the center-of-mass frame. The imaginary part of the self-energy is then given by

$$\text{Im} \Pi_D^{(\text{ff})}(s) = \text{Im} \Pi_D(s) F^2(|\vec{q}|), \quad (19)$$

$|\vec{q}| = (s - m_c^2)/(2\sqrt{s})$ , while the real part is determined by an unsubtracted dispersion integral. The bare meson mass is then adjusted to render a vanishing real part of the propagator at the physical resonance mass.

As default parameters for our calculations we use massless light quarks, a charm-quark mass of  $m_c = 1.5$  GeV and physical  $D$ -meson masses  $(m_D^{\text{phys}})^2 = m_D^2 - \text{Re} \Pi_D[(m_D^{\text{phys}})^2] = 2$  GeV (corresponding to a vanishing real part in the propagator). The coupling constant  $G \equiv G_{S,V}$  is varied to allow for widths of the  $D$ -meson spectral functions of 300-500 MeV, to approximately cover the range suggested by effective quark models [24, 25, 26]. It is important to note that we assume the  $D$ -meson resonances to be located *above* the  $c$ - $\bar{q}$  mass threshold,  $m_c + m_{\bar{q}}$ , which renders them accessible in  $c$ - $\bar{q}$  scattering processes. The situation is quite different for (bound) meson states (*i.e.*, below the anti-/quark threshold), where the resonant part of the scattering amplitude cannot be probed through  $c + \bar{q} \rightarrow c + \bar{q}$  interactions (even for resonance masses close to threshold, thermal energies of anti-/quarks imply that the average collision energy is significantly above the resonance peak). In this case, other processes need to be calculated, *e.g.*,  $c + \bar{q} \rightarrow D + g$ , where the extra gluon in the final state carries away 4-momentum to allow the  $D$ -meson to emerge on-shell. The same framework is also applied to the bottom sector, with  $b$ -quark and  $B$ -meson masses of  $m_b = 4.5$  GeV and  $m_B = 5$  GeV, respectively.

As we will see below, for equal on-shell masses and widths of the  $D$ -meson spectral functions, both regularization schemes lead to quite comparable results for the thermal relaxation properties of  $c$ -quarks, even though the off-shell properties differ significantly.

The  $D$ -meson propagators figure into the invariant matrix elements for elastic  $c$ -quark scattering off quarks,  $c + q \rightarrow c + q$ , and antiquarks,  $c + \bar{q} \rightarrow c + \bar{q}$ , in the  $u$ - and  $s$ -channel, respectively. One finds

$$\sum |\mathcal{M}_{\bar{q}}|^2 = 720G^4(s - m_c^2)^2 |D_D(s)|^2 \quad (20)$$

$$\sum |\mathcal{M}_q|^2 = 720G^4(u - m_c^2)^2 |D_D(u)|^2, \quad (21)$$

where we have summed over the contributions of all light-quark resonances, being equal due to either the heavy-quark symmetry ( $D$ - $D^*$ ,  $D_0^*$ - $D_1$ ) or chiral symmetry ( $D$ - $D_0^*$ ,  $D^*$ - $D_1$ ). We also included finite-mass strange quarks along with  $D_s$ - and  $D_s^*$ -mesons.

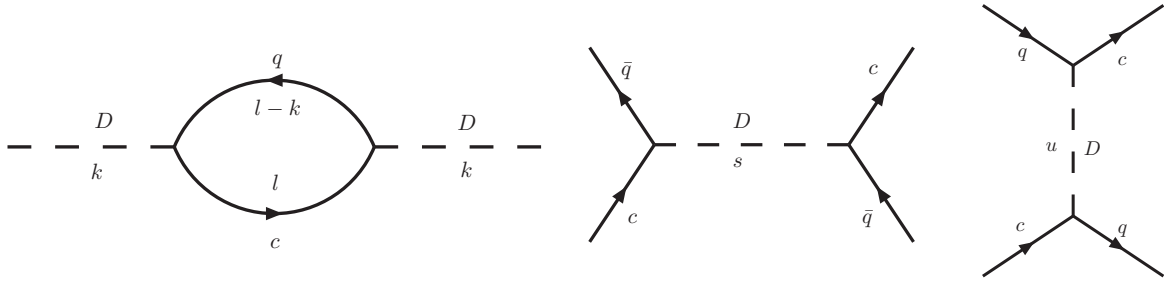


FIG. 1: Left panel:  $c(b)$ - $q$  loop diagram representing the  $D(B)$ -meson self-energy in the QGP. Right panel: "meson"-exchange diagrams contributing to the invariant matrix elements for the scattering of charm quarks on light quarks ( $u$ -channel) and anti-quarks ( $s$ -channel).

In addition to resonant interactions, elastic scattering in perturbative QCD is accounted for to leading order in  $\alpha_s$ ,  $\mathcal{O}(\alpha_s^2)$ . The corresponding matrix elements [21] have been supplemented with an additional gluon Debye (screening) mass,  $\mu_g = gT$ , which regulates the forward singularity in the  $t$ -channel exchange graphs [20]. The strong coupling constant will be varied over the range  $\alpha_s = 0.3-0.5$ .

### III. CHARM QUARK RESCATTERING IN THE QGP

#### A. Fokker-Planck Equation, Drag and Diffusion Coefficients

The above matrix elements are now implemented within a kinetic theory framework to assess the thermalization time scales for heavy quarks in a QGP. Following the steps outlined in Ref. [20], we start from the Boltzmann equation for the heavy-quark distribution function  $f(t, \vec{p})$  and neglect any mean-field terms. Furthermore assuming the scattering processes to be dominated by small momentum transfers one arrives at a Fokker-Planck equation describing the time evolution of  $f$  in momentum space,

$$\frac{\partial f(t, \vec{p})}{\partial t} = \frac{\partial}{\partial p_i} \left[ A_i(\vec{p}) + \frac{\partial}{\partial p_j} B_{ij}(\vec{p}) \right] f(t, \vec{p}) . \quad (22)$$

For an isotropic (rotationally invariant) plasma the drag and diffusion coefficients in (22) can be decomposed as

$$A_i(\vec{p}) = p_i A(|\vec{p}|) \quad (23)$$

$$B_{ij}(\vec{p}) = \left( \delta_{ij} - \frac{p_i p_j}{\vec{p}^2} \right) B_0(|\vec{p}|) + \frac{p_i p_j}{\vec{p}^2} B_1(|\vec{p}|) \quad (24)$$

with the scalar functions

$$A(|\vec{p}|) = \langle 1 \rangle - \frac{\langle \vec{p} \cdot \vec{p}' \rangle}{\vec{p}^2} \quad (25)$$

$$B_0(|\vec{p}|) = \frac{1}{4} \left[ \langle \vec{p}'^2 \rangle - \frac{\langle (\vec{p} \cdot \vec{p}')^2 \rangle}{\vec{p}^2} \right] \quad (26)$$

$$B_1(|\vec{p}|) = \frac{1}{2} \left[ \frac{\langle (\vec{p} \cdot \vec{p}')^2 \rangle}{\vec{p}^2} - 2 \langle \vec{p}' \cdot \vec{p} \rangle + \vec{p}^2 \langle 1 \rangle \right] . \quad (27)$$

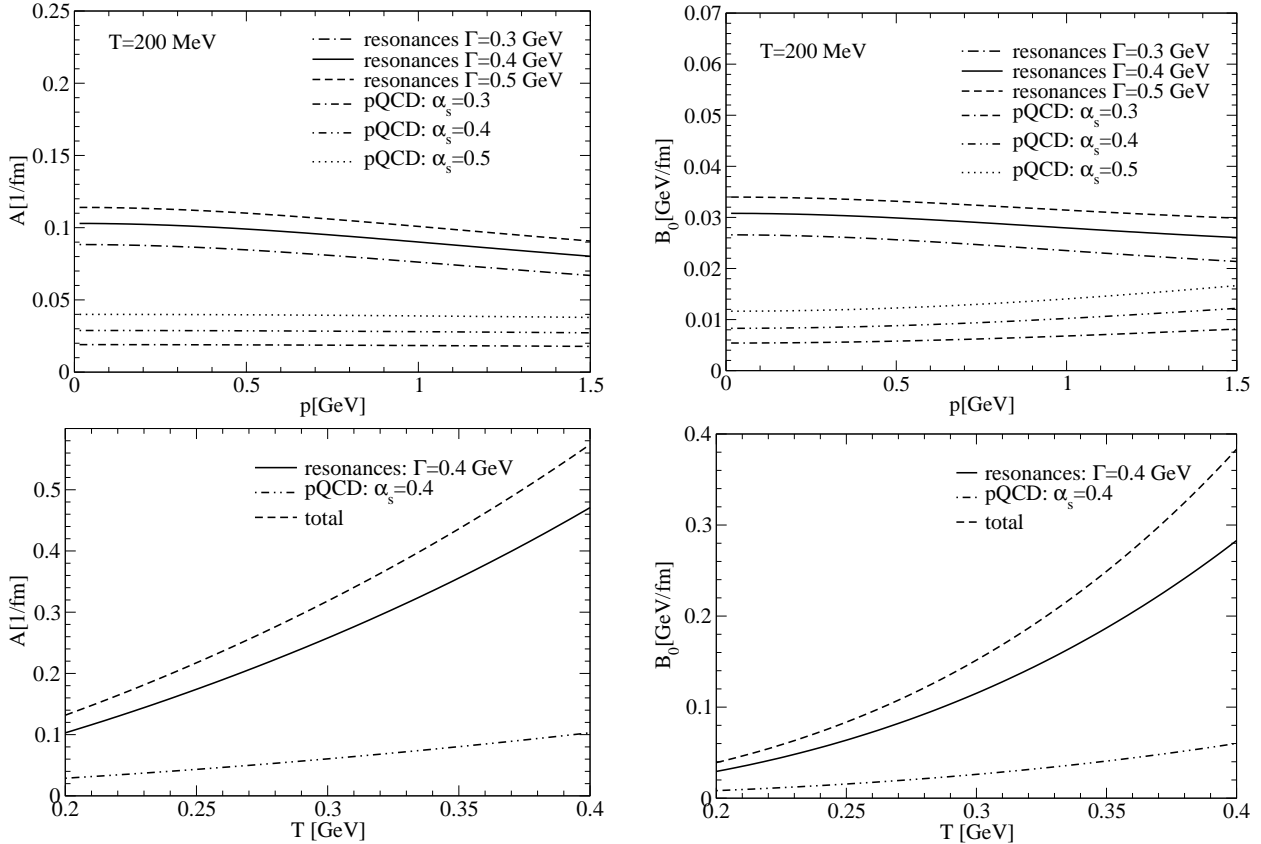


FIG. 2: Upper panel: drag coefficient  $A$  (left) and diffusion coefficient  $B_0$  (right) as a function of  $c$ -quark 3-momentum at a temperature of  $T = 200$  MeV for various values of  $\alpha_s$  (pQCD scattering) and  $D$ -meson widths (resonance exchanges). Lower panel: The same quantities as a function of temperature at fixed 3-momentum  $|\vec{p}| = 0$ .

The averaging is defined by

$$\langle X(\vec{p}') \rangle = \frac{1}{2E_p} \int \frac{d^3 \vec{q}}{(2\pi)^3 2E_q} \int \frac{d^3 \vec{q}'}{(2\pi)^3 2E_{q'}} \int \frac{d^3 \vec{p}'}{(2\pi)^3 2E_{p'}} \frac{1}{\gamma_c} \sum |\mathcal{M}|^2 \times (2\pi)^4 \delta^{(4)}(p + q - p' - q') \hat{f}(\vec{q}) X(\vec{p}') , \quad (28)$$

where  $\vec{p}$  ( $\vec{p}'$ ) and  $\vec{q}$  ( $\vec{q}'$ ) denote the momenta of the incoming (outgoing) charm- and light-quark/gluon, respectively, and  $\hat{f}(\vec{q})$  are the thermal Maxwell-Boltzmann distribution functions of the light partons. After integrating over the 4-momentum conserving  $\delta$ -function, and making use of Lorentz invariance of the matrix elements, the expressions for the scalar coefficients, Eqs. (25)-(27), can be reduced to numerically tractable 3-dimensional integrals<sup>2</sup>. The temperature and momentum dependencies of the  $A$  and  $B_0$  coefficients are summarized in Fig. 2. The main finding here is that for resonant rescattering both are increased by a substantial factor ( $\sim 3$ ) over the pQCD results (the latter are very similar to Ref. [20] as the extra factor of 2 is essentially compensated by the larger screening mass,  $\mu_g = gT$ , used in our calculation). The main reason for this effect is not so much an increase in the total cross section (the peak cross section in the resonance case of about 10 mb is comparable to an almost constant 4 mb for pQCD), but the isotropic angular

<sup>2</sup> We note that, when using the pQCD matrix elements, our final expressions are larger by a factor of 2 than the ones originally derived in Ref. [20].

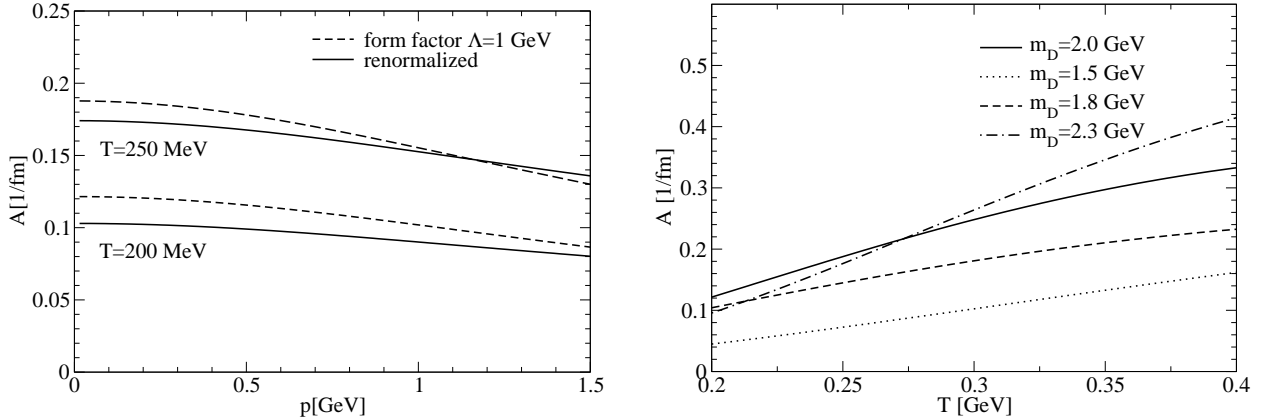


FIG. 3: Left panel: Comparison of the friction coefficient for resonances with self-energies calculated in the renormalization scheme (17) (solid line) and with form-factor regularization (dashed line). The coupling was chosen such that in both the resonance width  $\Gamma=0.4$  GeV at the resonance mass. Right panel: The friction coefficient for different resonance masses as function of the temperature, evaluated in the form-factor regularization scheme.

distribution of the resonance cross sections in contrast to forward dominated pQCD rescattering. Also note that the coefficients are rather insensitive to the underlying coupling constants for both resonance and pQCD scattering; naively, the matrix elements are proportional to the 4th power of the coupling constant, which would imply a variation by a factor of  $(5/3)^2 \simeq 2.6$  for the coefficients  $A$  and  $B_0$  for the parameter ranges shown in Fig. 2. The much smaller actual variation is due to compensating effects induced by an increased Debye mass for pQCD  $t$ -channel gluon exchange, and by an increased resonance width for  $s$ -channel  $D$ -meson exchange.

To further illustrate the uncertainties inherent to the resonance properties, in Fig. 3 we plot the sensitivity of the drag coefficient with respect to the regularization schemes and the resonance masses (for form-factor regularization). From the left panel one observes that the momentum dependence of the  $A$  coefficient is somewhat more pronounced for the form-factor regularization, but the absolute magnitude in both schemes is very similar. The right panel indicates a more pronounced sensitivity to the value of the resonance mass. In particular, it confirms that  $D$ -meson masses close to threshold lead to a significant reduction of the drag effect, due to the thermal motion of the light partons from the heat bath. For the same reason, larger masses imply a steeper increase of  $A$  with temperature (of course, above  $T \simeq 2T_c$  the very existence of resonance correlations is questionable).

## B. Time Evolution of Momentum Spectra

### 1. Time Dependence of the Fokker Planck Equation

To obtain a better estimate of the effect of heavy-quark rescattering on the transverse-momentum ( $p_T$ ) spectra of heavy-flavor hadrons in URHIC's we investigate in this section the time evolution of the Fokker-Planck equation in a thermally evolving QGP. The latter is modelled by an expanding fireball under conditions resembling central  $Au-Au$  collisions at RHIC. The main simplifying assumption consists of momentum-independent drag and diffusion coefficients. According to the discussion at the end of the previous section, we will therefore employ  $D$ -meson self-energies within the renormalization scheme (17) (with masses and widths of  $m_D=2$  GeV and  $\Gamma=0.4$  GeV), as well as pQCD cross sections (with  $\alpha_s=0.4$ ), cf. Fig. 2. The Fokker-Planck Eq. (22)

then takes the form

$$\frac{\partial f}{\partial t} = \gamma(t) \frac{\partial}{\partial \vec{p}}(\vec{p}f) + D(t) \frac{\partial^2}{\partial \vec{p}^2}f , \quad (29)$$

where  $\gamma = A(T(t), |\vec{p}| = 0)$  and  $D = B_0(T(t), |\vec{p}| = 0) = B_1(T(t), |\vec{p}| = 0)$ . The time dependence of the coefficients enters through their dependence on temperature (as determined in the previous section), with  $T(t)$  following from the fireball model outlined below. For the initial condition,

$$f(t = 0, \vec{p}) \equiv f_0(\vec{p}) , \quad (30)$$

we will employ  $c$ -quark spectra from  $p$ - $p$  collisions as extracted from the PYTHIA event generator [31, 32]. The initial-value problem can be conveniently solved employing Green's function techniques: if we can find a solution  $G(t, \vec{p}; \vec{p}_0)$  to Eq. (29) with the initial condition

$$G(t = 0, \vec{p}; \vec{p}_0) = \delta^{(3)}(\vec{p} - \vec{p}_0) , \quad (31)$$

the full solution with an arbitrary initial condition (30) follows as

$$f(t, \vec{p}) = \int d^3 \vec{p}_0 G(t, \vec{p}; \vec{p}_0) f_0(\vec{p}_0) . \quad (32)$$

To determine the Green's function, we define its Fourier transform,

$$G(t, \vec{p}; \vec{p}_0) = \int d^3 \vec{q} \exp(-i\vec{q} \cdot \vec{p}) g(t, \vec{q}; \vec{p}_0) , \quad (33)$$

and insert it into Eq. (29), leading to the first-order differential equation

$$\frac{\partial g}{\partial t} + \gamma \vec{q} \frac{\partial g}{\partial \vec{q}} = -D \vec{q}^2 g . \quad (34)$$

With the initial condition for  $g$  determined by Eq. (31),

$$g(0, \vec{q}, \vec{p}_0) = \frac{1}{(2\pi)^3} \exp(-i\vec{p}_0 \cdot \vec{q}) , \quad (35)$$

its solution reads

$$g(t, \vec{q}; \vec{p}_0) = \frac{1}{(2\pi)^3} \exp\{i\vec{p}_0 \cdot \vec{q} \exp[-\Gamma(t)]\} \exp[-\Delta(t)\vec{q}^2] , \quad (36)$$

where

$$\Gamma(t) = \int_0^t d\tau \gamma(\tau) \quad (37)$$

$$\Delta(t) = \exp[-2\Gamma(t)] \int_0^t d\tau D(\tau) \exp[2\Gamma(\tau)] . \quad (38)$$

The Fourier transformation (33) yields the result for the Green's function,

$$G(t, \vec{p}; \vec{p}_0) = \left[ \frac{1}{4\pi\Delta(t)} \right]^{3/2} \exp\left\{ -\frac{(\vec{p} - \vec{p}_0 \exp[-\Gamma(t)])^2}{4\Delta(t)} \right\} , \quad (39)$$

and the time evolution of the distribution function, Eq. (32), is finally obtained by numerical integration.

## 2. Limiting Cases

Before we turn to the full solution, let us first illustrate a few limiting cases. For time-independent coefficients  $\gamma$  and  $D$ , Eqs. (37) and (38) simplify to

$$\Gamma(t) = \gamma t, \quad \Delta(t) = \frac{D}{2\gamma} [1 - \exp(-2\gamma t)]. \quad (40)$$

Inserting these into Eq. (39) yields

$$G(t, \vec{p}; \vec{p}_0) = \left\{ \frac{\gamma}{2\pi D [1 - \exp(-2\gamma t)]} \right\}^{3/2} \exp \left\{ -\frac{\gamma}{2D} \frac{[\vec{p} - \vec{p}_0 \exp(-\gamma t)]^2}{1 - \exp(-2\gamma t)} \right\}, \quad (41)$$

which was already derived in Ref. [20]. This, in particular, shows that  $\gamma$  has the meaning of a drag (or friction) coefficient,

$$\langle \vec{p}(t) \rangle = \vec{p}_0 \exp(-\gamma t), \quad (42)$$

characterizing the equilibration time scale  $\tau = 1/\gamma$ . With the momentum fluctuation given by

$$\langle \vec{p}^2(t) \rangle - \langle \vec{p}(t) \rangle^2 = \frac{3D}{\gamma} [1 - \exp(-2\gamma t)], \quad (43)$$

$D$  is readily identified as a momentum diffusion coefficient. From the left panel of Fig. 4 we see that for temperatures expected in central *Au-Au* collisions at RHIC, the equilibration time scale for charm quarks is substantially reduced by resonant interactions, to about a few fm/ $c$ , comparable to the duration of the (putative) QGP phase. Even though a similar mechanism is operative for bottom quarks, their much larger rest mass renders the pertinent kinetic equilibration time significantly larger, around 10 fm/ $c$  or more.

For  $t \rightarrow \infty$ , Eq. (41) approaches a Maxwell-Boltzmann distribution,

$$\lim_{t \rightarrow \infty} G(t, \vec{p}; \vec{p}_0) = f_{\text{eq}}(\vec{p}) = \left( \frac{\gamma}{2\pi D} \right)^{3/2} \exp \left[ -\frac{\gamma \vec{p}^2}{2D} \right], \quad (44)$$

and thermal equilibrium implies the dissipation-fluctuation theorem,

$$T = \frac{D}{\gamma m_c}. \quad (45)$$

The such obtained temperature  $T$  should, of course, coincide with the one of the (light-quark and gluon) heat bath entering through the thermal distribution functions in Eq. (28). Thus, Eq. (45) serves as a consistency check for the determination of the drag and diffusion coefficients within our model, especially for the assumption on the dominance of small momentum transfers underlying the Fokker-Planck Equation (22). From the right panel in Fig. 4 we see that, for charm quarks, the dissipation-fluctuation theorem is well satisfied (within 3%) when using forward peaked pQCD cross sections; but also for the isotropic resonance cross sections within the renormalization scheme the deviations do not exceed 11% even at the highest considered temperatures, while within the form-factor regularization scheme they reach up to 26% (the latter value is reduced to  $\sim 17\%$  when an average over a thermal momentum distribution is performed). The latter finding can be explained by the greater variation of the friction and diffusion coefficients with momentum which makes the approximation of momentum-independent coefficients, underlying the derivation of the fluctuation-dissipation relation (45), less accurate. For this reason, in the next section we shall use the renormalization scheme without form factor to investigate the time evolution of  $p_T$  spectra. For the heavier bottom quarks the fluctuation-dissipation theorem is satisfied to high accuracy.

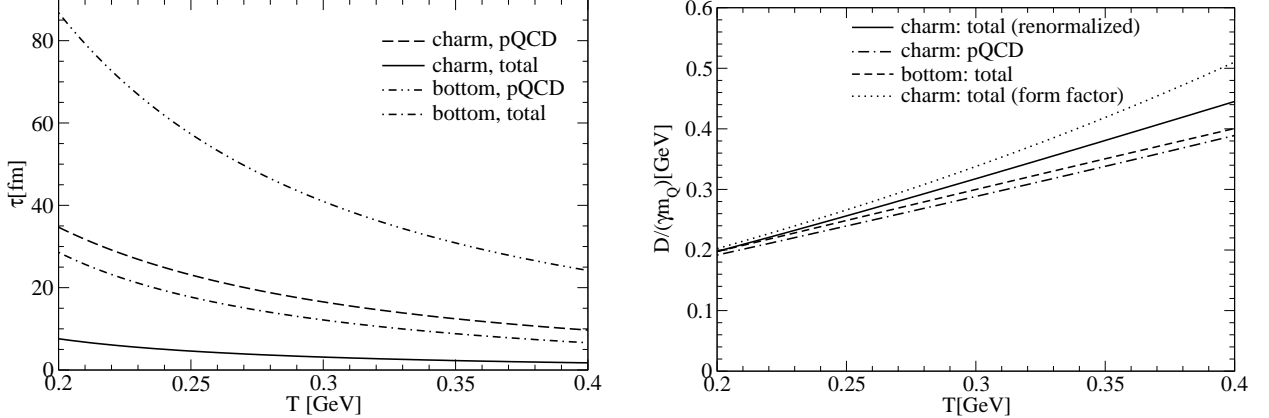


FIG. 4: Left panel: equilibration time-scale  $\tau = 1/\gamma$  for charm and bottom quarks in the QGP as function of temperature with (solid and dashed line) and without (dash-dotted and dash-double-dotted lines) in-medium resonances. Right panel: consistency check of the dissipation-fluctuation relation, Eq. (45), for  $c$ -quarks with (solid line) and without (dash-dotted line) resonances, as well as for  $b$ -quarks (with resonances, dashed line), in the QGP.

### 3. Charm-Quark $p_T$ Spectra at RHIC

Let us finally address the time evolution of charm-quark  $p_T$ -spectra including the temperature dependence of drag and diffusion coefficients. To obtain the time evolution of the temperature we use a simple expanding fireball model [33]. In reminiscence to hydrodynamic simulations [34] of central  $Au$ - $Au$  collisions at RHIC, the fireball volume is parameterized by

$$V_{FB}(t) = \pi(z_0 + v_z t)(r_0 + \frac{1}{2}a_{\perp}t^2)^2, \quad (46)$$

where  $r_0 = 6.5$  fm and  $z_0 = 0.6$  fm are the initial transverse and longitudinal size (the latter corresponding to a formation time of  $\tau_0 = 0.33$  fm/ $c$ ). The longitudinal and transverse expansion are characterized by  $v_z = 1.4c$  (covering a thermal width of about 1.8 units in rapidity) and  $a_{\perp} = 0.055 c^2/\text{fm}$  (yielding a total fireball lifetime of about 14 fm/ $c$  with a thermal freezeout temperature of  $\sim 110$  MeV).

Assuming isentropic expansion, the temperature at each instant is calculated from the total entropy of produced particles,  $S = s(T)V_{FB}(t) \simeq 10^4$  (within  $\Delta y = 1.8$ ), with the entropy density in the QGP given by

$$s = \frac{4\pi^2}{90} T^3 (16 + 10.5N_f), \quad (47)$$

( $N_f$  is the effective number of quark flavors, taken to be 2.5).

With these parameters, the initial QGP temperature is  $T_0 \simeq 375$  MeV, decreasing to the critical temperature of  $T_c \simeq 180$  MeV after about 3 fm/ $c$ , with further evolution in a hadron-QGP mixed phase for another 3 fm/ $c$ . For simplicity, we treat the latter phase as a QGP at constant  $T = T_c \simeq 180$  MeV, but accounting for lower parton densities as estimated from the temperature dependence of the Fokker-Planck coefficients (from the lower panel of Fig. 2 we estimated  $A, B \propto \rho^{1/2}$ ).

For the initial distribution  $f_0(\vec{p})$ , Eq. (30), we employ charm-quark  $p_T$ -spectra as generated in proton-proton ( $p$ - $p$ ) collisions at 200 GeV by PYTHIA [32]. A suitable parameterization thereof is

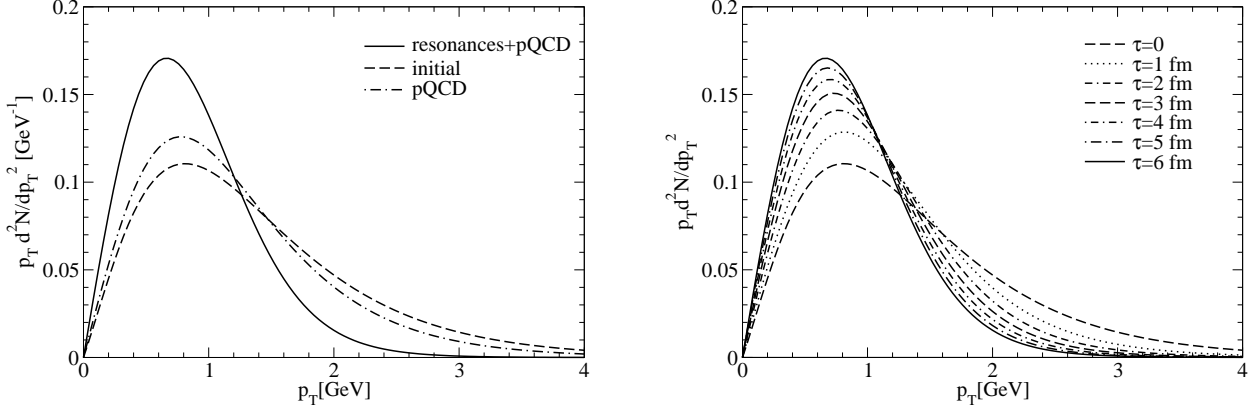


FIG. 5: Left panel: results for the time-evolved  $c$ -quark  $p_T$ -spectra in the local rest frame with a temperature profile corresponding to QGP and mixed phase in central  $Au$ - $Au$  at  $\sqrt{s_{NN}}=200$  GeV; dashed curve: initial spectrum taken from  $p$ - $p$  collisions; dash-dotted curve: final spectrum using pQCD cross sections only; solid curve: final spectrum using both pQCD and  $D$ -meson resonance interactions. Right panel: explicit time evolution in time steps of 1 fm/ $c$  for the pQCD+resonance interactions.

given by [31]

$$\frac{d^2N_c}{dp_T^2} = C \frac{(p_T + A)^2}{(1 + p_T/B)^\alpha} \quad (48)$$

with  $A = 0.5$  GeV,  $B = 6.8$  GeV,  $\alpha=21$ , and  $C = 0.845$ .

As detailed above, the time evolution of the  $p_T$  distribution is obtained from Eq. (32) with the Green's function (41), integrated over  $p_z$ , which amounts to a 2-dimensional solution of the Fokker-Planck equation. Fig. 5 summarizes our results for the time evolution of  $c$ -quark  $p_T$ -spectra in central  $Au$ - $Au$  at RHIC, evaluated in the local (thermal) rest frame of the expanding matter in QGP and mixed phase (*i.e.*, the additional boost from the collective transverse expansion is not included), using the drag and diffusion coefficients computed in Sec. III A. From the left panel one finds that, when allowing for pQCD rescattering only, the initial spectra from  $p$ - $p$  collisions are only affected rather little. On the contrary, when augmenting the interactions with  $D$ -meson resonances<sup>3</sup>, the  $p_T$  spectra undergo a marked reshaping, essentially a redistribution from high to low  $p_T$ . The final spectra (*i.e.*, at the end of the mixed phase after 6 fm/ $c$ ), with a peak position at  $p_T^{(\text{max})} \simeq 0.66$  GeV, indeed closely resemble a thermal distribution with a temperature of about 290 MeV. Even though this indicates that the spectra are not fully thermalized at  $T_c$ , the change from an initial average  $\sqrt{\langle p_T^2 \rangle} = 1.66$  GeV (corresponding to a “temperature” of  $\sim 920$  MeV) is appreciable. The fact that most of rescattering occurs in the early evolution phase (the first 3 fm/ $c$  or so, cf. right panel of Fig. 5) should provide favorable conditions for the build-up of *elliptic* flow.

We recall that our treatment is not reliable at high  $p_T$ , mainly for two reasons: (i) we have neglected the momentum dependence of the drag and diffusion coefficients, *i.e.*, used values at zero momentum, whereas in reality they decrease with  $p_T$ ; (ii) we have not included the (possibly gradual) disappearance of the resonance states towards high temperature, and the high- $p_T$  part is particularly sensitive to the early phases (see right panel of Fig. 5).

<sup>3</sup> Note that, when adding the matrix elements for pQCD and resonance interactions, we did not resum the perturbative contributions to, say,  $c + \bar{q} \rightarrow c + \bar{q}$  in the  $D$ -meson resonance propagator. In principle, this would lead to a slight renormalization of the resonance mass and width, which, however, is well inside the range of uncertainties of the in-medium resonance parameters.

#### IV. CONCLUSIONS AND OUTLOOK

In the present work we have studied the role of resonant rescattering for heavy quarks in a Quark-Gluon Plasma at moderate temperatures. Our main assumption has been the existence of  $D$ -meson-like resonance states above  $T_c$  which finds support in both effective quark models and recent QCD lattice calculations. The underlying Lagrangian embodied both chiral and heavy-quark symmetry where the latter has been essential to ensure conserved vector currents (for  $D^*$  resonances). Bare masses and coupling constants of the model have been adjusted to render one-loop resummed  $D$ -meson spectral functions reminiscent to more microscopic calculations.

Pertinent cross sections for resonant  $c$ -quark rescattering on light antiquarks in the heat bath have been applied within a Fokker-Planck equation to evaluate kinetic thermalization. Our main finding is that the introduction of resonances in the QGP leads to a substantial reduction of the equilibration-time scales (by a factor of  $\sim 3$ ) as compared to estimates based on perturbative interactions. To a large extent, this difference originates from the isotropy of the angular distributions for resonant scattering, as opposed to mostly forward scattering in pQCD, which importantly enters into the (angular-weighted) transport cross section. The reduced timescales are very reminiscent to expected QGP lifetimes in central  $Au$ - $Au$  collisions at RHIC. Consequently, time-evolved  $c$ -quark  $p_T$ -spectra exhibit a marked tendency towards thermalization in the resonance picture, whereas they are only little affected by pQCD rescattering alone. This should have important consequences for the build-up of elliptic flow of charmed hadrons.

Let us briefly discuss further ramifications and directions for future work. Clearly, the three-momentum dependence of the drag and diffusion coefficients, the effects of transverse flow and the evaluation of elliptic flow need to be addressed. Quasiparticle masses for light quarks and gluons should be introduced to make a closer connection to the QGP equation of state. The disappearance of the bound states needs to be accounted for, especially for applications at LHC with larger anticipated initial temperatures than at RHIC. Indeed, a key question that may eventually be answered by lattice QCD is whether  $D$ -meson (and other) resonances in the QGP exist, and, if so, whether they are located *above* the two-quark threshold, which renders them accessible for direct ( $c+\bar{q} \rightarrow c+\bar{q}$ ) scattering processes. Clearly, if this is not the case, other processes, such as  $c+\bar{q} \rightarrow D+g$ , need to be evaluated. The effects on secondary  $c\bar{c}$  production should also be checked. *E.g.*, according to recent transport calculations [23], upscaling pQCD cross sections by a factor of 3 (to generate a significant elliptic flow) entails an increase in open-charm pairs by 40-50% over primordial production in central  $Au$ - $Au$  collisions at RHIC, which is not supported by current PHENIX data [35]. Resonance cross sections, due to the larger  $D$ -meson mass in the crossed channel, may not have this feature (or, at least, to a less extent). Finally, we recall the important impact that heavy-quark momentum distributions have on secondary production (“coalescence”) of charmonium and bottomonium states. Obviously, the combined theoretical and experimental study of heavy-flavor probes promises a rich potential for the understanding of the complex nature of QGP at moderate temperatures.

#### Acknowledgments

One of us (HvH) thanks the Alexander von Humboldt foundation for support within a Feodor Lynen fellowship.

---

[1] R. Vogt, Phys. Rept. **310**, 197 (1999).

- [2] H. Satz, Rept. Prog. Phys. **63**, 1511 (2000).
- [3] R. Rapp and L. Grandchamp, J. Phys. **G30**, S305 (2004).
- [4] S. Batsouli, S. Kelly, M. Gyulassy, and J. L. Nagle, Phys. Lett. **B557**, 26 (2003).
- [5] V. Greco, C. M. Ko, and R. Rapp, Phys. Lett. **B595**, 202 (2004).
- [6] S. Kelly et al. (PHENIX Collaboration), J. Phys. **G30**, S1189 (2004).
- [7] F. Laue et al. (STAR Collaboration) (2004), nucl-ex/0411007.
- [8] E. V. Shuryak and I. Zahed, Phys. Rev. C **70**, 021901 (2004).
- [9] G. E. Brown, C.-H. Lee, M. Rho, and E. Shuryak, Nucl. Phys. **A740**, 171 (2004).
- [10] X. Li, H. Li, C. M. Shakin, and Q. Sun, Phys. Rev. **C69**, 065201 (2004).
- [11] S. Datta, F. Karsch, P. Petreczky, and I. Wetzorke, Nucl. Phys. Proc. Suppl. **119**, 487 (2003).
- [12] T. Umeda, K. Nomura, and H. Matsufuru (2002), hep-lat/0211003.
- [13] R. L. Thews, M. Schroedter, and J. Rafelski, Phys. Rev. C **63**, 054905 (2001).
- [14] B. Zhang, C. M. Ko, B.-A. Li, Z.-W. Lin, and S. Pal, Phys. Rev. C **65**, 054909 (2002).
- [15] L. Grandchamp, R. Rapp, and G. E. Brown, Phys. Rev. Lett. **92**, 212301 (2004).
- [16] P. Braun-Munzinger and J. Stachel, Phys. Lett. **B490**, 196 (2000).
- [17] M. I. Gorenstein, A. P. Kostyuk, H. Stocker, and W. Greiner, Phys. Lett. **B509**, 277 (2001).
- [18] R. L. Thews (2002), hep-ph/0206179.
- [19] L. Grandchamp and R. Rapp, Nucl. Phys. **A709**, 415 (2002).
- [20] B. Svetitsky, Phys. Rev. D **37**, 2484 (1988).
- [21] B. L. Combridge, Nucl. Phys. **B151**, 429 (1979).
- [22] L.-W. Chen and C. M. Ko (2004).
- [23] D. Molnar (2004), nucl-th/0410041.
- [24] F. O. Gottfried and S. P. Klevansky, Phys. Lett. **B286**, 221 (1992).
- [25] D. Blaschke, G. Burau, Y. L. Kalinovsky, and V. L. Yudichev, Prog. Theor. Phys. Suppl. **149**, 182 (2003).
- [26] D. Blaschke, G. Burau, T. Barnes, Y. Kalinovsky, and E. Swanson, Heavy Ion Phys. **18**, 49 (2003).
- [27] M. Asakawa and T. Hatsuda, Nucl. Phys. **A721**, C869 (2003).
- [28] D. Ebert, T. Feldmann, R. Friedrich, and H. Reinhardt, Nucl. Phys. **B434**, 619 (1995).
- [29] P. Ramond, *Field Theory: A Modern Primer* (Addison-Wesley, Redwood City, Calif., 1989), 2nd ed.
- [30] H. Georgi, Boulder TASI 91 pp. 589–630 (1991).
- [31] V. Greco, private communication.
- [32] T. Sjostrand, L. Lonnblad, S. Mrenna, et al., Comp. Phys. Commun. **135**, 238 (2001).
- [33] R. Rapp, Phys. Rev. C **63**, 054907 (2001).
- [34] P. F. Kolb and R. Rapp, Phys. Rev. C **67**, 044903 (2003).
- [35] S. S. Adler et al. (PHENIX Collaboration) (2004), nucl-ex/0409028.